Prediction of the bubble wall velocity for a large jump in degrees of freedom

Mikel Sanchez-Garitaonandia[1] and Jorinde van de Vis[2,3]

[1]*CPHT, CNRS, École polytechnique, Institut Polytechnique de Paris, 91120 Palaiseau, France*
[2]*Institute for Theoretical Physics, Utrecht University, Princetonplein 5, 3584 CC Utrecht, Netherlands*
[3]*Instituut-Lorentz for Theoretical Physics, Leiden University, Niels Bohrweg 2, 2333 CA Leiden, Netherlands*

(Received 2 February 2024; accepted 4 June 2024; published 9 July 2024)

The bubble expansion velocity is an important parameter in the prediction of gravitational waves from first-order phase transitions. This parameter is difficult to compute, especially in phase transitions in strongly coupled theories. In this work, we present a method to estimate the wall velocity for phase transitions with a large enthalpy jump, valid for weakly and strongly coupled theories. We find that detonations are disfavored in this limit, but wall velocities are not necessarily small. We also investigate the effect of two other features in the equation of state: nonconformal sound speeds and a limited range of temperatures for which the phases exist. We find that the former can increase the wall velocity for a given nucleation temperature, and the latter can restrict the wall velocities to small values. To test our approach, we use holographic phase transitions, which typically display these three features. We find excellent agreement with numerically obtained values of the wall velocity. We also demonstrate that the implications for gravitational waves can be significant.

DOI: 10.1103/PhysRevD.110.023509

I. INTRODUCTION

Many models for particle physics beyond the Standard Model (BSM) predict that one or more first-order phase transitions (PTs) might have occurred in the history of the Universe. These phase transitions might have played a role in the generation of the matter-antimatter asymmetry [1–8] or the production of dark matter [9–12]. First-order PTs can also source a gravitational wave (GW) signal when the released vacuum energy gets converted into sound waves, gradient energy in the bubble walls, and/or turbulence [13–16]. Depending on the strength and temperature of these transitions, the signals could be observable with the next generation of GW telescopes [17–19]. See, e.g., Refs. [19–22] for reviews.

Using GWs to learn about BSM physics requires accurate predictions of the GW spectrum. Analytical arguments and hydrodynamic simulations have resulted in a predicted GW spectrum as a broken power law [19,23–30]. The underlying assumption in Refs. [19,25–28,30], which was checked in Refs. [23,24], is that the amplitude of the signal can be predicted by the nucleation temperature T_n and rate β, wall velocity ξ_w, and sound speed c_s, as well as the so-called energy budget, that can be computed from the hydrodynamics of a single bubble.[1] In most cases, the energy budget can be estimated from the phase transition strength α, ξ_w [34], and c_s [35,36]. The challenge of predicting the GW spectrum is thus reduced to a computation of the thermal parameters and the hydrodynamics.

The wall velocity strongly affects the strength and shape of the GW spectrum [19,34], and it also enters in computations of the baryon asymmetry [37–42] or dark matter abundance [9–12]. It is, however, challenging to compute for a given theory (see, however, Refs. [43–47] for some explicit computations) and is therefore often treated as a free parameter, or simply set to $\xi_w \to 1$. This results in a significant uncertainty, so better estimates are necessary. Unfortunately, the difficulty of computing the wall velocity is even greater in strongly coupled theories [48–52], where a quasiparticle interpretation underlying the computations of Refs. [43–47] may not be available. In this work, we will provide a way to determine ξ_w that can be applied to both weakly and strongly coupled theories when they have a large jump in the number of degrees of freedom between the phases—we will refer to this as a large enthalpy jump. We will take a holographic equation of state (EOS) as an explicit example, which can be used to understand aspects of strongly coupled PTs [53,54]. Holographic models

[1]Strictly speaking, the GW signal should be computed at the percolation temperature T_p. Often, one can approximate $T_p \sim T_n$, but this assumption cannot always be made [31–33].

represent a useful playground where we can obtain insight into strongly coupled cosmological PTs [55–61] and possibly into PTs in neutron star mergers [62]. It has already been shown that ξ_w can be obtained in a holographic PT [63–66], and we can use these results to test our approach.

Holographic theories are characterized by a gravitational description that is dual to a strongly coupled gauge theory with a large number N of degrees of freedom. They naturally exhibit three distinctive features (see, e.g., Refs. [67,68]):

(i) a large jump in enthalpy between the high-temperature and low-temperature phase,
(ii) a limited range of temperature for which the phases exist,
(iii) strong deviation in the sound speed from the conformal value $c_s^2 = 1/3$.

We will see that these features can strongly modify the hydrodynamic predictions compared to the often-made assumptions that $c_s^2 \sim 1/3$ and that the temperature can take any value.[2] We also stress that these features are not unique to holographic PTs and that our results apply to nonholographic models as well.

The main result of this work is a demonstration that the wall velocity for models with a large enthalpy jump follows directly from the EOS and the nucleation temperature, without further details of the plasma. Some steps in this direction were already taken in Ref. [66], in which a formula was proposed to obtain the wall speed for planar bubbles. Our results are valid for spherical bubbles, and we will compare our results for planar bubbles with the findings there. Additionally, detonations are not realizable in the infinite enthalpy jump limit. If the allowed temperature range is limited, we find that the resulting wall velocity is rather small, favoring deflagrations as observed in Refs. [63,64,66], and likely excluding detonations. Finally, we will see that quantitative results can get strongly affected by a nonconformal sound speed. GW predictions for models with a large enthalpy jump get significant corrections compared to the "vanilla" assumption where ξ_w is a free parameter and $c_s^2 = 1/3$.

II. HYDRODYNAMIC AND THERMODYNAMIC DESCRIPTION OF BUBBLE EXPANSION

A. Hydrodynamics

Finding the kinetic energy in the fluid requires solving the hydrodynamic equations of a single expanding bubble. We will summarize the approach here, and further details can be found in Refs. [16,34,69,70]. The hydrodynamic equations follow from the energy-momentum tensor of a perfect fluid,

$$T^{\mu\nu} = w u^\mu u^\nu - p g^{\mu\nu}, \tag{1}$$

where $w = T dp/dT$ is the enthalpy. $g^{\mu\nu}$ denotes the metric, which is assumed to be the Minkowski metric, and $u^\mu = \gamma(1, \vec{v})$ denotes the fluid velocity with $\gamma = 1/\sqrt{1-\vec{v}^2}$. The hydrodynamic equations for u^μ and w are obtained by projecting $\partial_\mu T^{\mu\nu} = 0$ in the direction parallel and perpendicular to the fluid flow,

$$\begin{aligned} 2\frac{v}{\xi} &= \gamma^2(1-v\xi)\left[\frac{\mu^2(\xi,v)}{c_s^2} - 1\right]\partial_\xi v, \\ \partial_\xi w &= w\left(1+\frac{1}{c_s^2}\right)\gamma^2\mu(\xi,v)\partial_\xi v, \end{aligned} \tag{2}$$

where $\xi = r/t$ (with r the radial distance to the center of the bubble and t the time since nucleation), v is the fluid velocity in radial coordinates, and μ is the Lorentz-boosted velocity, $\mu(\xi, v) = (\xi - v)/(1 - \xi v)$. The speed of sound follows from p via

$$c_s^2 = \frac{dp/dT}{de/dT}, \qquad e = p\frac{dp}{dT} - p. \tag{3}$$

The only regions where this hydrodynamic description fails are the bubble walls and shocks. Nevertheless, given their small size compared to the bubble, they can be replaced by discontinuities across which we impose matching conditions, that are obtained by integration $\partial_\mu T^{\mu\nu} = 0$ from right behind the wall/shock to right in front of the wall/shock, yielding

$$\begin{aligned} w_+ v_+^2\gamma_+^2 + p_+ &= w_- v_-^2\gamma_-^2 + p_-, \\ w_+ v_+\gamma_+^2 &= w_- v_-\gamma_-^2, \end{aligned} \tag{4}$$

where the $+, (-)$ label denotes quantities evaluated right in front of (behind) the discontinuity. After some algebraic manipulations, we obtain

$$v_+ v_- = \frac{p_+ - p_-}{e_+ - e_-}, \qquad \frac{v_+}{v_-} = \frac{e_- + p_+}{e_+ + p_-}, \tag{5}$$

for the matching conditions. Note that the velocities are defined with respect to the frame of the wall/shock.

By solving Eqs. (2) and imposing the matching conditions (5) at the wall and possible shock, we can solve for the whole flow as a function of two input parameters, e.g., ξ_w and T_n (or, similarly, α_n). The energy budget K is determined from the ratio of the fluid kinetic energy to the enthalpy of the high-temperature phase at T_n. For each T_n, there are three type of solutions depending on the value of

[2]Sometimes this assumption is implicit, by using an approximation for the energy budget of Refs. [34–36]. The underlying models of Refs. [34–36] exist for arbitrary temperatures, and the corresponding solutions could probe temperatures unrealistically far away from T_n.

the wall speed with respect to the sound speed (see, e.g., Ref. [34]):

(i) Deflagrations: $\xi_w < c_{s,L}$. In this case, $v_- = \xi_w$ and $v_+ < c_{s,H}(T_+)$.
(ii) Hybrids: $c_{s,L} < \xi_w < v_J$, with v_J the Jouguet velocity (see, e.g., Refs. [34,70,71]). We now have $v_- = c_{s,L}$ and $v_+ <= c_{s,H}$.
(iii) Detonations: $\xi_w > v_J$, with $v_- > c_{s,L}$ and $v_+ = \xi_w$.

Here and in the following, we use the subscript H (L) for quantities defined in the high- (low-)enthalpy phase.

B. Equations of state

We will consider three equations of state to investigate the effects of large enthalpy jumps, temperature limitations, and $c_s^2 \neq 1/3$ on the hydrodynamic solutions. Let us parametrize the large enthalpy jump by some large number N and assume that low-enthalpy phase quantities are suppressed by[3] $1/N^2$.

1. Dark SU(N) model

We consider the model of Refs. [53,54], which is based on a holographic description of a confinement/deconfinement PT. The thermodynamic equation of state can be obtained following the approach described in Ref. [53], which we will not repeat here, but we demonstrate the pressure and sound speed of the high-enthalpy phase in Fig. 1. We see that the sound speed deviates strongly from $c_s^2 = 1/3$. At the nucleation temperature $T_n = 0.993 T_c$ [60], $c_s^2 = 0.103$. Note that the model only describes the high-enthalpy phase, which ceases to exist at $T < T_{\mathrm{min,SU(N)}}$. Even though we leave N as a free parameter, the model implicitly assumes that N is large, as contributions that are smaller than $\mathcal{O}(N^2)$ are neglected. For the low-enthalpy phase, we will assume the equation of state proposed by Ref. [72] (although we will find that nothing depends on this for large N),

$$p_L = \frac{1}{N^2}\frac{T_c^4}{\nu - 1}\left(\frac{T}{T_c}\right)^{\nu}, \tag{6}$$

where the sound speed is a constant set by $\nu = 1 + 1/c_{s,L}^2$, which parametrizes the unknown equation of state of the low-enthalpy phase.

2. Template model

We use the model of Ref. [72] to describe models with constant, but nonconformal sound speeds,

[3]The inspiration for this suppression factor comes from confining holographic and large-N gauge theories, where the high-enthalpy phase has N^2 degrees of freedom and the low-enthalpy phase has $\mathcal{O}(1)$. However, we do not take any other assumptions from holography, so the results we obtain are general for models with a large enthalpy jump.

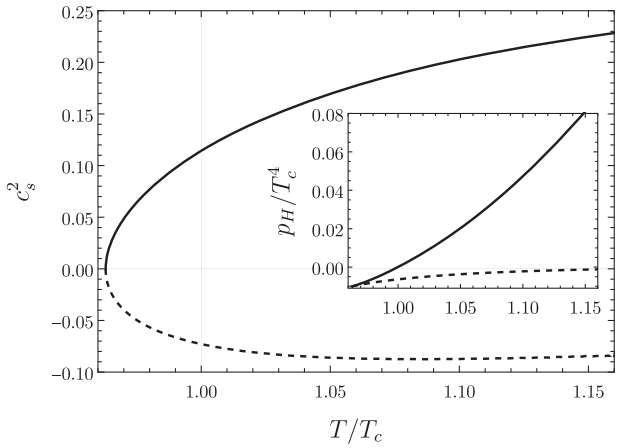

FIG. 1. Speed of sound squared and pressure (inset) of the high enthalpy phase. The dashed lines correspond to states that are thermodynamically unstable.

$$p_H = \frac{a_H T_c^4}{\mu - 1}\left(\frac{T}{T_c}\right)^{\mu} - \epsilon,$$
$$p_L = \frac{1}{N^2}\frac{a_H T_c^4}{\nu - 1}\left(\frac{T}{T_c}\right)^{\nu}, \tag{7}$$

where and $\mu = 1 + 1/c_{s,H}^2$ and a_H parametrizes the number of degrees of freedom of the high-enthalpy phase and ϵ is a temperature-independent constant, which parametrizes the energy difference between the two phases. The virtue of the template model is that it allows us to study the effect of the nonconformal sound speed and large enthalpy jump, without the limited temperature range. The often-used bag equation of state is a special case of the template model with $\mu = \nu = 4$.

In all cases, we assume that the low-enthalpy phase temperature cannot grow as large as to undo the $1/N^2$ suppression; i.e., we assume that $T_L \ll T_c N^{2/\nu}$.

3. Strongly coupled holographic model

We will briefly discuss the model of Ref. [64] in Sec. III C, a holographic description of a strongly coupled phase transition with $N \sim 3$ (see Ref. [64] for details). The bubble wall velocity of this model was determined in Ref. [63], and we will compare it to our estimate.

III. HYDRODYNAMICS WITH A LARGE ENTHALPY JUMP

A. Matching conditions in the large-N limit

Let us consider the matching conditions of Eq. (5) in the limit of $N \to \infty$. Given the suppression that we assumed for the low-enthalpy phase, the following ratios hold,

$$\frac{w_-}{w_+} \sim \frac{s_-}{s_+} \sim \frac{e_-}{e_+} \sim \frac{1}{N^2}, \tag{8}$$

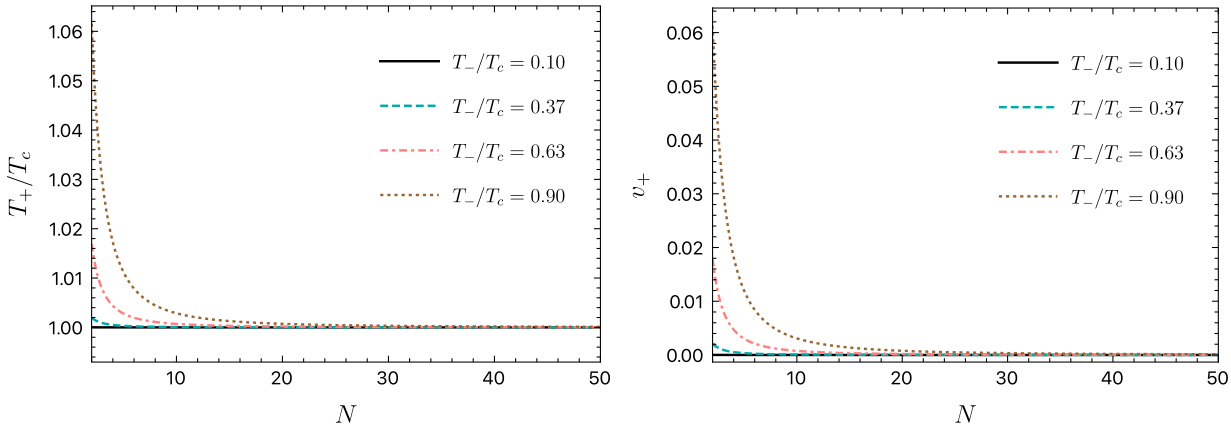

FIG. 2. T_+/T_c (left) and v_+ (right) as a function of N for different choices of T_-. T_+ tends to T_c, and v_+ tends to zero as N increases, regardless of T_-.

where $s = w/T$. We have assumed the previously mentioned bound on the low-enthalpy phase temperature.

The relation between the pressures of both phases is more complicated. By the definition of T_c, $p_H(T_c) = p_L(T_c)$, which means that p_-/p_+ does not need to be small. Indeed,

$$\frac{p_-}{p_+} \sim \frac{1}{N^2} \quad \text{if} \quad \frac{|T_+ - T_c|}{T_c} \gg \frac{1}{N^2}, \qquad \text{case 1},$$
$$\frac{p_-}{p_+} \sim 1 \quad \text{if} \quad \frac{|T_+ - T_c|}{T_c} \lesssim \frac{1}{N^2}, \qquad \text{case 2}. \tag{9}$$

We will now study the matching conditions for these two different cases.

Case 1 Let us first investigate Eq. (5) with $p_-/p_+ \sim 1/N^2$,

$$v_+ v_- \sim \frac{p_+}{e_+}\left(1 + \mathcal{O}\left(\frac{1}{N^2}\right)\right) \sim \frac{v_+}{v_-}, \tag{10}$$

with solution[4] $v_- = 1 - \mathcal{O}(1/N^2)$, which corresponds to a detonation, as we have seen in Sec. II A. In a detonation, $v_+ > v_-$, so Eq. (4) implies that $w_- > w_+$, which is not possible in the large-N limit.[5]

Case 2 If $p_-/p_+ \sim 1$, then

$$v_+ v_- = \mathcal{O}\left(\frac{1}{N^2}\right), \qquad \frac{v_+}{v_-} = \mathcal{O}\left(\frac{1}{N^2}\right), \tag{11}$$

implying that $v_+ = \mathcal{O}(1/N^2)$, corresponding to a deflagration or a hybrid. In combination with Eq. (9), this leads to the following conditions for a large enthalpy jump bubble expansion,

$$T_+ = T_c \quad \text{and} \quad v_+ = 0. \tag{12}$$

The condition on v_+ was already stated in Ref. [66] and it was also pointed out there that the condition on T_+ was a good approximation for the simulations presented in Refs. [63,66].

Let us point out that the matching relation just obtained does not restrict us to slow walls, as the Jouguet velocity, which is the transition from hybrids to detonations, can become arbitrarily close to unity for a large amount of supercooling (see, e.g., Ref. [34]).

We conclude that large enthalpy jump PTs lead to deflagrations or hybrids characterized by the condition (12) while detonations are excluded.

B. Hydrodynamic solutions

We expect the matching relations of Eq. (12) to hold in any theory with a large enthalpy jump, but in order to use them to find the relation between ξ_w and T_n requires a solution of the hydrodynamic equations in the shock wave. This requires an EOS, and the relation between ξ_w and T_n will be numerical.

In this section, we solve the hydrodynamics for the dark SU(N) and the template model [with $c_s^2 = 1/3$ and $c_s^2 = 0.103$—the same value as in the dark SU(N)], for increasing N.

Let us focus first on deflagrations and hybrids. We demonstrate in the left panel of Fig. 2 that T_+ indeed approaches T_c, independent of the choice of T_-. The slower converge for larger T_- is to be expected as we require larger N to suppress the enthalpy at higher temperatures. Similarly, v_+ approaches 0 as N increases, independently of the value of T_-, as shown in the right panel of Fig. 2. We used the template model with $\mu, \nu = 4$ but have confirmed explicitly that the convergence also occurs for other sound speeds and the dark SU(N) model.

The lines of Fig. 3 demonstrate the relation $\xi_w(T_n)$ obtained from solving the hydrodynamic equations with the

[4]Note that we use the sign conventions of Ref. [34], in which all velocities are positive.

[5]Even without taking the large-N limit, detonations can be excluded in certain theories with a limited temperature range as having $w_- > w_+$ may not be possible.

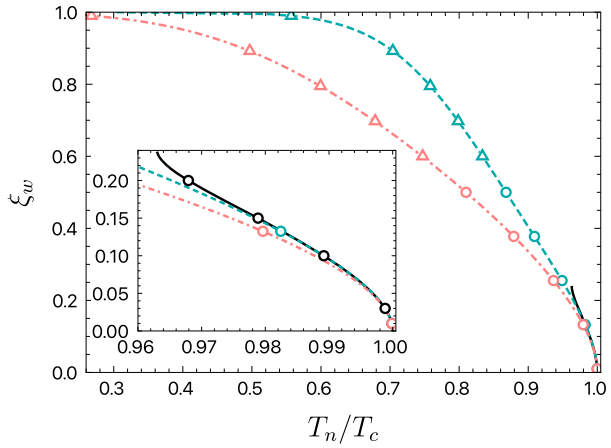

FIG. 3. Wall speed as a function of the nucleation temperature in the dark SU(N) model (black), template model with $c_s^2 = 1/3$ (pink dot-dashed), and with $c_s^2 = 0.103$ (cyan dashed). Circles correspond to deflagrations and triangles to hybrids.

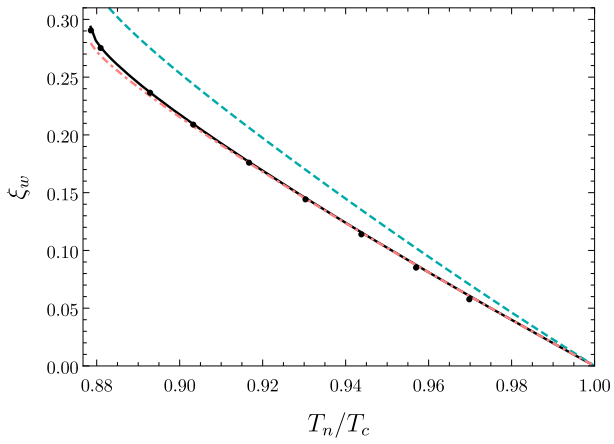

FIG. 4. Wall speed from the simulations in Ref. [63] (dots) and the result using the condition (12) (solid black), local thermal equilibrium (dashed cyan), and the simple wave formula (14) (dot-dashed pink).

matching conditions of Eq. (12). In this limit, the solution is obtained without any reference to the fluid behind the wall. The dots demonstrate the result for $N = 30$ (with $\nu = 4$ and $T_-/T_c = 0.5$), and we see that they agree extremely well. We observe that for the holographic model only solutions with $\xi_w \lesssim 0.25$ exist. The reason becomes immediately clear: the minimum temperature of the high-enthalpy phase prevents further supercooling. From the results of the template model, we see that when such a minimum temperature does not exist there is—in principle—no limit on the amount of supercooling, and the wall velocity can grow arbitrarily large. This is a very important observation, as it suggests that the low wall velocities found in real-time holographic simulations [63,64,66] are not a result of the strongly coupled nature of these theories, but rather of the impossibility of strong supercooling.

Another interesting observation is that the sound speed strongly affects the relation between T_n and ξ_w. For models with $c_s^2 < 1/3$, the typical velocity is larger than for $c_s^2 = 1/3$, and a smaller amount of supercooling is required for a fast wall, in agreement with Ref. [66].

Finally, we checked that detonations get excluded in the large enthalpy jump limit for the template model. Given a fixed ξ_w and T_n, Eq. (5) implies that p_- and e_- are independent of N, meaning that the temperature scales as $T_- \propto T_c N^{2/\nu}$ for detonations. But this corresponds precisely to the range of temperatures that we excluded in the large-N limit because it undoes the $1/N^2$ suppression.

C. Comparison with the strongly coupled holographic model

Let us now put our result to the test, by comparing to the wall velocity obtained in an actual simulation. Figure 4 demonstrates a comparison to the values of ξ_w obtained in the strongly coupled holographic model in Ref. [63] for planar bubbles. In this case, $\partial_\mu T^{\mu\nu} = 0$ reduces to $\partial_\xi v = \partial_\xi w = 0$ for deflagrations, and one only has to solve the matching conditions at the shock.

We see that the large enthalpy jump description (solid black) already gives a very accurate estimate of the wall velocity, even though N is only approximately 3. We also compare the result to the wall velocity obtained assuming local thermal equilibrium at the bubble wall (dashed cyan) [71,73,74], and interestingly this gives a comparable estimate, albeit somewhat larger. This can be understood in the large enthalpy jump limit as follows. The entropy change at the wall, in the wall frame, is given by

$$s_H(T_+)\gamma_+ v_+ - s_L(T_-)\gamma_- v_- \to 0, \tag{13}$$

which vanishes due to $v_+ \to 0$ and $s_- \to 0$ when $N \to \infty$. This is exactly the condition for local thermal equilibrium, and we would therefore expect an even better agreement between the two approaches for larger N.

Additionally, we display the prediction of the simple wave (SW) formula [66] (pink dot-dashed), with the additional assumption $v_+ = 0$ and $T_+ = T_c$,

$$\xi_w = \tanh \int_{T_n}^{T_c} \frac{dT}{T c_s}. \tag{14}$$

Notice that the results are very close to ours for $T_n \sim T_c$, but start disagreeing for smaller T_n. This effect can be perfectly understood in the template model, where both approaches offer analytical results,

$$\xi_w^{\text{large } N} = \frac{c_{s,H}(T_c^\mu - T_n^\mu)}{\sqrt{(T_c^\mu + c_{s,H}^2 T_n^\mu)(T_n^\mu + c_{s,H}^2 T_c^\mu)}},$$
$$\xi_w^{\text{sw}} = \tanh\left(\frac{1}{c_{s,H}} \log \frac{T_c}{T_n}\right), \tag{15}$$

with $\mu = 1 + 1/c_{s,H}^2$. The series expansions of both expressions around $T_n = T_c$ agree perfectly to second order. However, greater discrepancy with the data is expected for theories with stronger supercooling.

IV. IMPLICATIONS FOR GWS

Let us now discuss the possible implications for the GW spectrum, taking the dark SU(N) model and the template model as concrete examples. For the prediction of the GW spectrum, we first follow the approach of Ref. [19], and then further discuss its applicability.

In Ref. [60], the GW spectrum of the dark SU(N) model was predicted for three different values of the wall velocity $\xi_w = (0.01, 0.1, 1)$, for a nucleation temperature of $T_n/T_c \sim 0.993$ (note that $T_n \sim T_p$ holds in this model). Using the given nucleation temperature, we find that the correct wall velocity is $\xi_w = 0.078$ in the large enthalpy limit (which is implicitly used in Ref. [60], by assuming that the low-enthalpy phase can be ignored). The sound speed deviates strongly from $c_s^2 = 1/3$ (see Fig. 1), and we take its full effect on the energy budget into account in the dashed cyan line in Fig. 5, using $\beta/H = 6.4 \times 10^4$ and $T_c = 100$ GeV from Ref. [60]. For comparison, we also show in solid black the GW prediction for $c_s^2 = 1/3$ like was done in Ref. [60]. We see that the effect of the nonconformal sound speed is to increase the peak frequency by almost a factor 2 and to reduce the peak amplitude by a factor ∼2 (largely due to the explicit c_s in the GW amplitude). If we now compare to the GW predictions of Ref. [60], we conclude that the large enthalpy jump fixes the velocity to a relatively small value, reducing the GW signal compared to more optimistic choices. Moreover, we see that the deviation in c_s significantly affects the signal. For concreteness, we compared our result with $\xi_w = 0.078$ and the full temperature-dependent c_s and find a suppression of a factor ∼80 compared to the $\xi_w = 1$, $c_s^2 = 1/3$ result obtained in Ref. [60], demonstrated by the black dotted line.

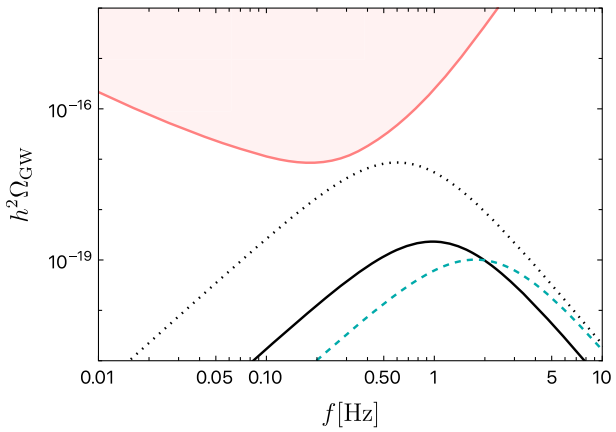

FIG. 5. Prediction of the GW signal in models with a large enthalpy jump and $T_c = 100$ GeV. The two lower lines show the dark SU(N), with $T_n/T_c = 0.993$ and ξ_w computed in the large-N limit. The dashed cyan line considers the full model, and the black solid line assumed that $c_s^2 = 1/3$. The black dotted line shows the spectrum if one assumes $\xi_w = 1$ and $c_s^2 = 1/3$. The pink area shows the power-law-integrated sensitivity curve of the future GW experiment Big Bang Observer [75–77], obtained from Ref. [78].

Although it looks like the GW spectrum could be significantly enhanced by allowing for a larger amount of supercooling, and correspondingly larger ξ_w, we refrain from giving such a prediction here. The reason is that the simulations of Refs. [23,24] on which the GW predictions of Ref. [19] are based never probed large values of α corresponding to such supercooling. Moreover, the vacuum energy domination would trigger a period of inflation [79,80], which affects the GW spectrum.

The GW prediction for models with a large enthalpy jump might even need further revision, due to the large amount of latent heat $L = e_H - e_L \sim e_H$ released. As discussed in Refs. [13,81–83], for phase transitions with large amount of latent heat *and* a small amount of supercooling, the nucleation and growth of bubbles gets delayed due to heating of the plasma by the first generation of nucleated bubbles, suppressing the GW amplitude.[6] The extent of this effect is possibly model dependent, as a large amount of latent heat does not need to imply a small amount of supercooling. In Refs. [58,85], it was demonstrated that the amount of supercooling in (holographic) models with a large number of degrees of freedom can in fact be large.

Another effect that likely modifies the GW spectrum was observed in the simulations of Ref. [86]. For strong deflagrations, bubble walls were observed to slow down before colliding, due to the formation of heated droplets of the high-temperature phase. This caused a vortical component in the fluid field and a suppression of the kinetic energy compared to the predictions of Ref. [19]. Reference [56] included this suppression in the prediction of the GW spectrum from a holographic model and concluded that the spectrum from parameter points with small ξ_w became largely unobservable (by TianQin). Whether the suppression persists for larger phase transition strengths and/or fast hybrid walls is a matter that requires further study.

V. CONCLUSION

In this work, we have explored the consequences of a large enthalpy jump, limited allowed temperature range, and strong deviations from $c_s^2 = 1/3$ on the wall velocity and the predicted GW spectrum. Although these features arise naturally in holographic and strongly coupled

[6]In Ref. [84], $\xi_w < 10^{-6}$ was found in this scenario, but note that the amount of supercooling was significantly smaller than the one found in Ref. [60].

theories, our results are also applicable to weakly coupled theories.

A large enthalpy jump highly constrains the fluid flow, favoring deflagrations and hybrids over detonations, which cease to exist as the jump grows larger. It forces the fluid ahead of the wall to be at the critical temperature $T_+ = T_c$ and to move at the same speed as the wall, $v_+ = 0$. By integrating the hydrodynamic equations (2) and solving matching conditions at the shock, we showed that one can obtain a relation between the wall speed and the nucleation temperature depending solely on the EOS. Our estimate for the wall velocity becomes more accurate as the enthalpy jump increases in a given theory, as demonstrated in Fig. 3. The method can be applied to bubbles in arbitrary dimensions. A formula to obtain ξ_w was also proposed in Ref. [66], but it has not yet been generalized beyond planar bubbles, and it only agrees with our result in the regime of small supercooling.

As discussed around Eq. (13), the large-N limit also enforces local thermal equilibrium. This implies that as long as the enthalpy jump is large the estimate of ξ_w by the code snippet of Ref. [71] (developed for local thermal equilibrium) will be very similar to the one obtained with the method presented in this work.

We have pointed out that a limit on the amount of supercooling, rather than strong coupling, is the main limiting factor in obtaining fast walls. This clarifies the reason behind the low speeds measured in holographic simulations [63,64,66]. For illustration, we have computed the GW spectrum in the dark SU(N) model. We found that the limited temperature range indeed results in a small wall speed, which suppressed the GW spectrum compared to the choice $\xi_w = 1$. We also demonstrated that nonconformal values of c_s, which naturally occur in holographic models, significantly affect the GW spectrum.

Our main conclusion is that care is needed when determining the wall speed in the computation of the GW spectrum. We have demonstrated a way of estimating the wall velocity in the case of a large enthalpy jump, which can even be applied to strongly coupled theories and which should decrease the uncertainty in the GW prediction associated to ξ_w.

ACKNOWLEDGMENTS

We thank Fëanor Reuben Ares, Yann Gouttenoire, Oscar Henriksson, Mark Hindmarsh, Carlos Hoyos, Niko Jokela, Benoit Laurent, Francesco Nitti, and Nicklas Ramberg for discussions. We are grateful to Yago Bea for extensive discussions and to Romuald Janik for clarifications on the simple wave formula. The work of M. S. G. is supported by the European Research Council (ERC) under the European Union's Horizon 2020 research and innovation program (Grant No. 758759). J. v. d. V. is supported by the Dutch Research Council (NWO), under Project No. VI.Veni.212.133.

[1] V. A. Kuzmin, V. A. Rubakov, and M. E. Shaposhnikov, On the anomalous electroweak baryon number nonconservation in the early universe, Phys. Lett. B **155**, 36 (1985).
[2] M. E. Shaposhnikov, Possible appearance of the baryon asymmetry of the universe in an electroweak theory, JETP Lett. **44**, 465 (1986).
[3] M. E. Shaposhnikov, Baryon asymmetry of the universe in standard electroweak theory, Nucl. Phys. **B287**, 757 (1987).
[4] A. G. Cohen, D. B. Kaplan, and A. E. Nelson, Weak scale baryogenesis, Phys. Lett. B **245**, 561 (1990).
[5] A. G. Cohen, D. B. Kaplan, and A. E. Nelson, Progress in electroweak baryogenesis, Annu. Rev. Nucl. Part. Sci. **43**, 27 (1993).
[6] A. Katz and A. Riotto, Baryogenesis and gravitational waves from runaway bubble collisions, J. Cosmol. Astropart. Phys. 11 (2016) 011.
[7] I. Baldes, S. Blasi, A. Mariotti, A. Sevrin, and K. Turbang, Baryogenesis via relativistic bubble expansion, Phys. Rev. D **104**, 115029 (2021).
[8] A. Azatov, M. Vanvlasselaer, and W. Yin, Baryogenesis via relativistic bubble walls, J. High Energy Phys. 10 (2021) 043.
[9] M. J. Baker, J. Kopp, and A. J. Long, Filtered dark matter at a first order phase transition, Phys. Rev. Lett. **125**, 151102 (2020).
[10] D. Chway, T. H. Jung, and C. S. Shin, Dark matter filtering-out effect during a first-order phase transition, Phys. Rev. D **101**, 095019 (2020).
[11] A. Azatov, M. Vanvlasselaer, and W. Yin, Dark matter production from relativistic bubble walls, J. High Energy Phys. 03 (2021) 288.
[12] I. Baldes, Y. Gouttenoire, and F. Sala, Hot and heavy dark matter from a weak scale phase transition, SciPost Phys. **14**, 033 (2023).
[13] E. Witten, Cosmic separation of phases, Phys. Rev. D **30**, 272 (1984).
[14] A. Kosowsky, M. S. Turner, and R. Watkins, Gravitational radiation from colliding vacuum bubbles, Phys. Rev. D **45**, 4514 (1992).
[15] A. Kosowsky, M. S. Turner, and R. Watkins, Gravitational waves from first order cosmological phase transitions, Phys. Rev. Lett. **69**, 2026 (1992).
[16] M. Kamionkowski, A. Kosowsky, and M. S. Turner, Gravitational radiation from first order phase transitions, Phys. Rev. D **49**, 2837 (1994).

[17] C. Grojean and G. Servant, Gravitational waves from phase transitions at the electroweak scale and beyond, Phys. Rev. D **75**, 043507 (2007).
[18] C. Caprini and D. G. Figueroa, Cosmological backgrounds of gravitational waves, Classical Quantum Gravity **35**, 163001 (2018).
[19] C. Caprini *et al.*, Detecting gravitational waves from cosmological phase transitions with LISA: An update, J. Cosmol. Astropart. Phys. 03 (2020) 024.
[20] D. J. Weir, Gravitational waves from a first order electroweak phase transition: A brief review, Phil. Trans. R. Soc. A **376**, 20170126 (2018); **381**, 20230212(E) (2023).
[21] M. B. Hindmarsh, M. Lüben, J. Lumma, and M. Pauly, Phase transitions in the early universe, SciPost Phys. Lect. Notes **24**, 1 (2021).
[22] P. Athron, C. Balázs, A. Fowlie, L. Morris, and L. Wu, Cosmological phase transitions: From perturbative particle physics to gravitational waves, Prog. Part. Nucl. Phys. **135**, 104094 (2024).
[23] M. Hindmarsh, S. J. Huber, K. Rummukainen, and D. J. Weir, Numerical simulations of acoustically generated gravitational waves at a first order phase transition, Phys. Rev. D **92**, 123009 (2015).
[24] M. Hindmarsh, S. J. Huber, K. Rummukainen, and D. J. Weir, Shape of the acoustic gravitational wave power spectrum from a first order phase transition, Phys. Rev. D **96**, 103520 (2017); **101**, 089902(E) (2020).
[25] M. Hindmarsh, Sound shell model for acoustic gravitational wave production at a first-order phase transition in the early Universe, Phys. Rev. Lett. **120**, 071301 (2018).
[26] M. Hindmarsh and M. Hijazi, Gravitational waves from first order cosmological phase transitions in the sound shell model, J. Cosmol. Astropart. Phys. 12 (2019) 062.
[27] R. Jinno, T. Konstandin, and H. Rubira, A hybrid simulation of gravitational wave production in first-order phase transitions, J. Cosmol. Astropart. Phys. 04 (2021) 014.
[28] R. Jinno, T. Konstandin, H. Rubira, and I. Stomberg, Higgsless simulations of cosmological phase transitions and gravitational waves, J. Cosmol. Astropart. Phys. 02 (2023) 011.
[29] R.-G. Cai, S.-J. Wang, and Z.-Y. Yuwen, Hydrodynamic sound shell model, Phys. Rev. D **108**, L021502 (2023).
[30] A. Roper Pol, S. Procacci, and C. Caprini, Characterization of the gravitational wave spectrum from sound waves within the sound shell model, Phys. Rev. D **109**, 063531 (2024).
[31] J. Ellis, M. Lewicki, and J. M. No, On the maximal strength of a first-order electroweak phase transition and its gravitational wave signal, J. Cosmol. Astropart. Phys. 04 (2019) 003.
[32] P. Athron, C. Balázs, and L. Morris, Supercool subtleties of cosmological phase transitions, J. Cosmol. Astropart. Phys. 03 (2023) 006.
[33] P. Athron, L. Morris, and Z. Xu, How robust are gravitational wave predictions from cosmological phase transitions?, J. Cosmol. Astropart. Phys. 05 (2024) 075.
[34] J. R. Espinosa, T. Konstandin, J. M. No, and G. Servant, Energy budget of cosmological first-order phase transitions, J. Cosmol. Astropart. Phys. 06 (2010) 028.
[35] F. Giese, T. Konstandin, and J. van de Vis, Model-independent energy budget of cosmological first-order phase transitions—A sound argument to go beyond the bag model, J. Cosmol. Astropart. Phys. 07 (2020) 057.
[36] F. Giese, T. Konstandin, K. Schmitz, and J. van de Vis, Model-independent energy budget for LISA, J. Cosmol. Astropart. Phys. 01 (2021) 072.
[37] D. Bodeker, L. Fromme, S. J. Huber, and M. Seniuch, The Baryon asymmetry in the standard model with a low cut-off, J. High Energy Phys. 02 (2005) 026.
[38] L. Fromme, S. J. Huber, and M. Seniuch, Baryogenesis in the two-Higgs doublet model, J. High Energy Phys. 11 (2006) 038.
[39] J. De Vries, M. Postma, and J. van de Vis, The role of leptons in electroweak baryogenesis, J. High Energy Phys. 04 (2019) 024.
[40] J. M. Cline and K. Kainulainen, Electroweak baryogenesis at high bubble wall velocities, Phys. Rev. D **101**, 063525 (2020).
[41] G. C. Dorsch, S. J. Huber, and T. Konstandin, On the wall velocity dependence of electroweak baryogenesis, J. Cosmol. Astropart. Phys. 08 (2021) 020.
[42] J. M. Cline and B. Laurent, Electroweak baryogenesis from light fermion sources: A critical study, Phys. Rev. D **104**, 083507 (2021).
[43] G. D. Moore and T. Prokopec, How fast can the wall move? A study of the electroweak phase transition dynamics, Phys. Rev. D **52**, 7182 (1995).
[44] G. C. Dorsch, S. J. Huber, and T. Konstandin, Bubble wall velocities in the standard model and beyond, J. Cosmol. Astropart. Phys. 12 (2018) 034.
[45] M. Lewicki, M. Merchand, and M. Zych, Electroweak bubble wall expansion: Gravitational waves and baryogenesis in standard model-like thermal plasma, J. High Energy Phys. 02 (2022) 017.
[46] B. Laurent and J. M. Cline, First principles determination of bubble wall velocity, Phys. Rev. D **106**, 023501 (2022).
[47] S. Jiang, F. P. Huang, and X. Wang, Bubble wall velocity during electroweak phase transition in the inert doublet model, Phys. Rev. D **107**, 095005 (2023).
[48] P. Schwaller, Gravitational waves from a dark phase transition, Phys. Rev. Lett. **115**, 181101 (2015).
[49] S. Bruggisser, B. Von Harling, O. Matsedonskyi, and G. Servant, Electroweak phase transition and baryogenesis in composite Higgs models, J. High Energy Phys. 12 (2018) 099.
[50] W.-C. Huang, M. Reichert, F. Sannino, and Z.-W. Wang, Testing the dark SU(N) Yang-Mills theory confined landscape: From the lattice to gravitational waves, Phys. Rev. D **104**, 035005 (2021).
[51] J. Halverson, C. Long, A. Maiti, B. Nelson, and G. Salinas, Gravitational waves from dark Yang-Mills sectors, J. High Energy Phys. 05 (2021) 154.
[52] H. Yang, F. F. Freitas, A. Marciano, A. P. Morais, R. Pasechnik, and J. a. Viana, Gravitational-wave signatures of chiral-symmetric technicolor, Phys. Lett. B **830**, 137162 (2022).
[53] U. Gursoy, E. Kiritsis, L. Mazzanti, and F. Nitti, Holography and thermodynamics of 5D dilaton-gravity, J. High Energy Phys. 05 (2009) 033.

[54] U. Gursoy, E. Kiritsis, L. Mazzanti, and F. Nitti, Improved holographic Yang-Mills at finite temperature: Comparison with data, Nucl. Phys. **B820**, 148 (2009).
[55] F. Bigazzi, A. Caddeo, A. L. Cotrone, and A. Paredes, Fate of false vacua in holographic first-order phase transitions, J. High Energy Phys. 12 (2020) 200.
[56] F. R. Ares, M. Hindmarsh, C. Hoyos, and N. Jokela, Gravitational waves from a holographic phase transition, J. High Energy Phys. 21 (2020) 100.
[57] F. Bigazzi, A. Caddeo, A. L. Cotrone, and A. Paredes, Dark holograms and gravitational waves, J. High Energy Phys. 04 (2021) 094.
[58] F. R. Ares, O. Henriksson, M. Hindmarsh, C. Hoyos, and N. Jokela, Effective actions and bubble nucleation from holography, Phys. Rev. D **105**, 066020 (2022).
[59] Z.-R. Zhu, J. Chen, and D. Hou, Gravitational waves from holographic QCD phase transition with gluon condensate, Eur. Phys. J. A **58**, 104 (2022).
[60] E. Morgante, N. Ramberg, and P. Schwaller, Gravitational waves from dark SU(3) Yang-Mills theory, Phys. Rev. D **107**, 036010 (2023).
[61] Y. Chen, D. Li, and M. Huang, Bubble nucleation and gravitational waves from holography in the probe approximation, J. High Energy Phys. 07 (2023) 225.
[62] J. Casalderrey-Solana, D. Mateos, and M. Sanchez-Garitaonandia, Mega-hertz gravitational waves from neutron star mergers, arXiv:2210.03171.
[63] Y. Bea, J. Casalderrey-Solana, T. Giannakopoulos, D. Mateos, M. Sanchez-Garitaonandia, and M. Zilhão, Bubble wall velocity from holography, Phys. Rev. D **104**, L121903 (2021).
[64] Y. Bea, J. Casalderrey-Solana, T. Giannakopoulos, A. Jansen, D. Mateos, M. Sanchez-Garitaonandia, and M. Zilhão, Holographic bubbles with Jecco: Expanding, collapsing and critical, J. High Energy Phys. 09 (2022) 008; 03 (2023) 225(E).
[65] F. Bigazzi, A. Caddeo, T. Canneti, and A. L. Cotrone, Bubble wall velocity at strong coupling, J. High Energy Phys. 08 (2021) 090.
[66] R. A. Janik, M. Jarvinen, H. Soltanpanahi, and J. Sonnenschein, Perfect fluid hydrodynamic picture of domain wall velocities at strong coupling, Phys. Rev. Lett. **129**, 081601 (2022).
[67] Y. Bea and D. Mateos, Heating up exotic RG flows with holography, J. High Energy Phys. 08 (2018) 034.
[68] D. Elander, A. F. Faedo, D. Mateos, and J. G. Subils, Phase transitions in a three-dimensional analogue of Klebanov-Strassler, J. High Energy Phys. 06 (2020) 131.
[69] L. D. Landau and E. M. Lifshitz, *Fluid Mechanics* (Pergamon Press, New York, 1989).
[70] H. Kurki-Suonio and M. Laine, Supersonic deflagrations in cosmological phase transitions, Phys. Rev. D **51**, 5431 (1995).
[71] W.-Y. Ai, B. Laurent, and J. van de Vis, Model-independent bubble wall velocities in local thermal equilibrium, J. Cosmol. Astropart. Phys. 07 (2023) 002.
[72] L. Leitao and A. Megevand, Hydrodynamics of phase transition fronts and the speed of sound in the plasma, Nucl. Phys. **B891**, 159 (2015).
[73] M. Barroso Mancha, T. Prokopec, and B. Swiezewska, Field-theoretic derivation of bubble-wall force, J. High Energy Phys. 01 (2021) 070.
[74] W.-Y. Ai, B. Garbrecht, and C. Tamarit, Bubble wall velocities in local equilibrium, J. Cosmol. Astropart. Phys. 03 (2022) 015.
[75] J. Crowder and N. J. Cornish, Beyond LISA: Exploring future gravitational wave missions, Phys. Rev. D **72**, 083005 (2005).
[76] V. Corbin and N. J. Cornish, Detecting the cosmic gravitational wave background with the big bang observer, Classical Quantum Gravity **23**, 2435 (2006).
[77] G. M. Harry, P. Fritschel, D. A. Shaddock, W. Folkner, and E. S. Phinney, Laser interferometry for the big bang observer, Classical Quantum Gravity **23**, 4887 (2006); **23**, 7361(E) (2006).
[78] K. Schmitz, New sensitivity curves for gravitational-wave signals from cosmological phase transitions, J. High Energy Phys. 01 (2021) 097.
[79] T. Hambye, A. Strumia, and D. Teresi, Super-cool dark matter, J. High Energy Phys. 08 (2018) 188.
[80] I. Baldes and C. Garcia-Cely, Strong gravitational radiation from a simple dark matter model, J. High Energy Phys. 05 (2019) 190.
[81] K. Enqvist, J. Ignatius, K. Kajantie, and K. Rummukainen, Nucleation and bubble growth in a first order cosmological electroweak phase transition, Phys. Rev. D **45**, 3415 (1992).
[82] C. Alcock, G. M. Fuller, and G. J. Mathews, The quark—hadron phase transition and primordial nucleosynthesis, Astrophys. J. **320**, 439 (1987).
[83] P. Asadi, E. D. Kramer, E. Kuflik, G. W. Ridgway, T. R. Slatyer, and J. Smirnov, Thermal squeezeout of dark matter, Phys. Rev. D **104**, 095013 (2021).
[84] Y. Gouttenoire, E. Kuflik, and D. Liu, Heavy baryon dark matter from SU(N) confinement: Bubble wall velocity and boundary effects, Phys. Rev. D **109**, 035002 (2024).
[85] Y. Bea, J. Casalderrey-Solana, T. Giannakopoulos, A. Jansen, S. Krippendorf, D. Mateos, M. Sanchez-Garitaonandia, and M. Zilhão, Spinodal gravitational waves, arXiv:2112.15478.
[86] D. Cutting, M. Hindmarsh, and D. J. Weir, Vorticity, kinetic energy, and suppressed gravitational wave production in strong first order phase transitions, Phys. Rev. Lett. **125**, 021302 (2020).